

Journal of Materials Chemistry A

Accepted Manuscript



This is an *Accepted Manuscript*, which has been through the Royal Society of Chemistry peer review process and has been accepted for publication.

Accepted Manuscripts are published online shortly after acceptance, before technical editing, formatting and proof reading. Using this free service, authors can make their results available to the community, in citable form, before we publish the edited article. We will replace this *Accepted Manuscript* with the edited and formatted *Advance Article* as soon as it is available.

You can find more information about *Accepted Manuscripts* in the [Information for Authors](#).

Please note that technical editing may introduce minor changes to the text and/or graphics, which may alter content. The journal's standard [Terms & Conditions](#) and the [Ethical guidelines](#) still apply. In no event shall the Royal Society of Chemistry be held responsible for any errors or omissions in this *Accepted Manuscript* or any consequences arising from the use of any information it contains.

Cite this: DOI: 10.1039/c0xx00000x

www.rsc.org/xxxxxx

Working Mechanism and Performance of Polypyrrole as Counter Electrode for Dye-Sensitized Solar Cells

Shan Lu,^{a,b,c} Shasha Wang,^a Ruobing Han,^a Ting Feng,^d Lingju Guo,^a Xuehua Zhang,^{*a} Dongsheng Liu^{*c} and Tao He^{*a}

Received (in XXX, XXX) Xth XXXXXXXXX 20XX, Accepted Xth XXXXXXXXX 20XX

DOI: 10.1039/b000000x

Many different materials have been being used as the alternative counter electrodes (CEs) for dye-sensitized solar cells (DSSCs) mainly due to the high cost of Pt CEs. So far the majority of reported work just focuses on the modulation of conductivity and morphology of the CEs. The working mechanism is still unclear, specifically about the electrocatalysis. Here it is elucidated for the first time by using polypyrrole (PPy) as the target material. The electrocatalysis is mainly comprised of formation of the weakly and strongly bonded iodine species, and formation and reduction of the intermediates. This mechanism may be valid for other CEs too. We envision that this work can help to better understand and optimize the performance of DSSCs fabricated using alternative CEs.

1. Introduction

The DSSCs have been being widely studied due to overall low cost, high theoretical energy conversion efficiency, concise fabrication, and good flexibility.¹⁻⁶ The CE plays an important role in the DSSCs because it collects electrons flowing from external circuit and catalyzes regeneration of the mediator (usually Γ/I_3^- redox couple). Hence, the CE materials should have a low resistance and high electrocatalytic activity for Γ/I_3^- redox reaction.⁷ The Pt CE remains the stalwart due to its high catalytic activity and low charge transfer resistance.⁸ However, its high cost and low abundance have restricted the mass production of DSSCs. Moreover, the dissolution of Pt in Γ/I_3^- electrolyte deteriorates long term stability of the DSSCs.⁹ Thus, Pt-free materials with low cost and corrosion resistant have been developed, mainly based on transition metal and carbon materials.¹⁰⁻¹⁴ Recently organic conducting polymer has become another promising alternative, such as polyaniline, polypyrrole, poly(3,4-ethylenedioxythiophene), and their derivatives, due to their diversity in structure, high conductivity, good chemical stability, ready synthesis, non-toxic, low cost, and in favor of large-scale (flexible) device fabrication.¹⁵⁻¹⁸

So far the majority of research about the alternative CEs mainly focuses on the modulation of morphology and conductivity via changing the preparation protocol.¹⁰⁻²² However, the working mechanism is still unclear, specifically about electrocatalysis of the mediator regeneration on the CEs, which is critical for the design and development of the alternative CEs. As a matter of fact, only the working mechanism of Pt CE has been studied among all of the CEs.²³ The I_3^- ions originate from the electrolyte via diffusion or are generated on the Pt CE, which can

be reduced therein. It is suggested that the I(Pt) intermediate may be formed on the Pt CE.

Herein, the working mechanism of the alternative CEs is studied by using polypyrrole (PPy) as the target material. The PPy thin films can be porous in nature, which is in favor of ion diffusion. Moreover, the existing states of counter ions on the CEs can be relatively easily determined using polymer, which can help to probe the working mechanism. The proposed mechanism is different from the one for the Pt CE. It may be valid for other CEs too, not just for PPy CEs. This will provide a better understanding about the application of alternative CEs in the DSSCs, especially when Γ/I_3^- redox couple is used as the mediator.

2. Experimental

Preparation of PPy CEs: The PPy thin films were prepared at room temperature by electrochemical polymerization on FTO substrates ($1.2 \times 1.5 \text{ cm}^2$, $14 \Omega \square^{-1}$) with a CHI 660D potentiostat (CH Instrument) under a constant bias of 0.75 V for 80 s in an aqueous solution containing 0.1 M pyrrole monomer, 10 mM LiI and different concentrations of TsOH (0.1, 0.5, 1.0, and 2.0 M). The respective pH value of the polymerization solution is 1.53, 0.98, 0.75, and 0.63, respectively. Electrochemical polymerization is used because it has many advantages such as controllable initiation and termination of polymerization, low-temperature and fast process. The TsOH and LiI are used as supporting electrolyte. Moreover, TsO^- is one of the most popular doping anions.²⁴ Since Γ/I_3^- redox couple is the most popular mediator in the DSSCs, the introduction of iodine species into the PPy is used to probe the working mechanism of the CEs. A Pt sheet ($1 \times 1 \text{ cm}^2$) and a saturated calomel electrode (SCE) were

used as counter and reference electrode, respectively.

Fabrication of DSSCs: The sandwich-type DSSCs were fabricated. TiO₂ photoanode was prepared on FTO by using doctor-blade technique with TiO₂ paste (13 nm, Wuhan Geao Co., Ltd.), followed by sintering at 70, 125, 325, 375, 450, and 500 °C for 7, 10, 15, 10, 15, and 10 min, respectively. Then they were treated with 20 mM TiCl₄ aqueous solution at 70 °C for 30 min and were sintered again at 450 °C for 30 min on a hot plate. After being cooled down to 80 °C, they were immersed for about 12 h in a mixture solution of acetonitrile and t-butanol (volume ratio of 1:1) containing 0.5 mM D149 dye and 1 mM deoxycholic acid. The resultant dye-sensitized (D149) TiO₂ film was used as working electrode and an as-prepared PPy film was used as CE in DSSCs. The electrolyte solution in the DSSCs contains 50 mM I₂, 0.1 M LiI, 0.6 M 1-methy-3-propylimidazolium iodide (DMPIIm), 0.5 M 4-tert-butylpyridine (TBP) and 3-methoxypropionitrile (3-MPN).

Characterizations and measurements: The surface morphology and thickness of PPy films were studied by FE-SEM Hitachi S-4800. The absorption spectra were collected with an UV/Vis/NIR spectrophotometer, Perkin-Elmer Lambda 750. Electrochemical impedance spectra (EIS) of the DSSCs with different PPy CEs were obtained in dark using CHI660D electrochemical station under a range of 0.01 Hz ~ 100 kHz. XPS spectra were obtained on an AXIS ULTRA^{DL} instrument (Kratos) and the data were analyzed using Vision2 software. Electrochemical properties of the films were characterized by cyclic voltammetry (CV) measurements with a CHI660D electrochemical station in acetonitrile electrolyte containing 0.1 M LiClO₄, 10 mM LiI and 1 mM I₂. The effective electrochemical active surface area was evaluated by double-layer capacitance using the same electrolyte as CV, which was performed with a small amplitude triangle wave linear scan using. The photocurrent-voltage (*J-V*) characteristics of the DSSCs were measured with a solar simulator (Model 69907, Oriel) and a Keithley source meter (2420) under illumination of AM 1.5G light with an intensity of 85 mW cm⁻².

3. Results and discussion

3.1. Photovoltaic performance of DSSCs based on PPy CEs

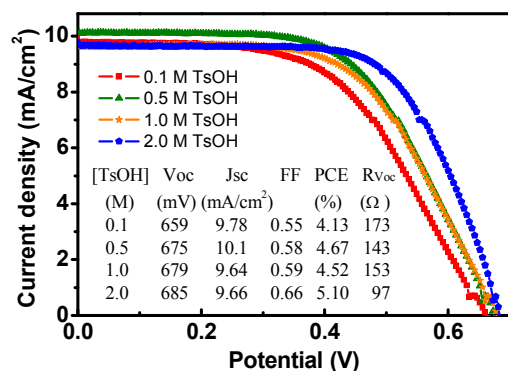


Fig. 1 J-V curves of DSSCs assembled with PPy thin film CEs prepared with 0.1 M pyrrole, 10 mM LiI and different TsOH concentration of 0.1, 0.5, 1.0, and 2.0 M, respectively.

Fig. 1 shows photocurrent-voltage (*J-V*) curves of the DSSCs

based on different PPy CEs. It is found that the open circuit voltage (V_{OC}) and fill factor (FF) increase with increasing concentration of TsOH used for the preparation of PPy CEs; while the internal resistance (R_{VOC}) decreases, except a slight increase at 1.0 M. In addition, it is noted that the max V_{OC} in this work is lower than some results reported previously, which may be because the dye used here is D149, instead of the popular N719 for the TiO₂ photoanodes. The short circuit current density (J_{SC}) first increases with increasing concentration of TsOH, while it decreases again and hardly changes when the concentration is 1.0 M and above. A similar trend is also observed for the J_{SC} derived from the results of monochromatic incident photon-to-current conversion efficiency (IPCE) measurements (Supporting Information). The power conversion efficiency (PCE) increases with the increase of TsOH concentration, except a slight decrease at 1.0 M. The highest PCE of 5.10% is obtained for DSSC based on PPy CE prepared with electrolyte solution containing 2.0 M TsOH. All these have been explained in light of the morphology, conductivity and electrocatalytic properties of the CEs. The working mechanism is proposed accordingly. In addition, the PPy films exhibit relatively good stability since only slight change can be observed after cyclic voltammetry (CV) scanning at both room temperature and 80 °C (Supporting Information), indicating the PPy films can be used as the CEs for the DSSCs.

3.2. Morphology of PPy thin films

The morphology of the PPy films was observed by SEM images (**Fig. 2a-f**). The presence of TsOH and Γ ions in the polymerization solution can influence the topographic feature of the PPy films. The bulk film is comprised of dense PPy nanoparticles, regardless of the presence of Γ ions. The surface of PPy film polymerized without Γ ions is relatively flat and smooth (**Fig. 2e**), while some granular protuberance are formed on the film surface when Γ ions are used. It is suggested that the electrochemical and chemical oxidation can contribute concurrently to the polymerization due to the presence of both doping anions and oxidative iodine species in the solution (**Fig. 2g**). The former occurs at the interface of electrolyte and solid (FTO substrate in the beginning and PPy film later), while the latter takes place where the oxidative iodine species exist. The observed change in solution color before and after polymerization is ascribed to the consumption of iodine species via both processes. In the initial stage, the electrochemical polymerization plays a major role and results in the formation of a relatively dense thin film adjacent to the substrate. The films exhibit similar morphology when the TsOH concentration is relatively low, such as 0.5 M and below. The small granular particles observed at moderate concentration (such as 1.0 M) disappear when it increases to 2.0 M. This is because the polymer particles formed electrochemically and chemically interweave with each other, leading to the formation of a porous structure atop the initial dense film. A porous network is almost completed at 2.0 M.

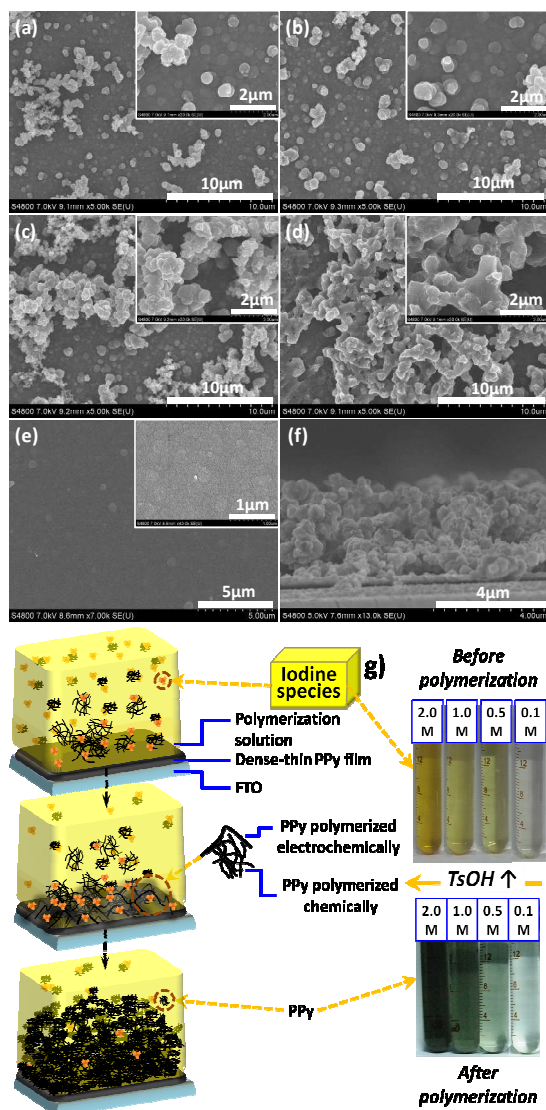


Fig. 2 SEM images of as-prepared PPy films polymerized in aqueous solution containing 0.1 M pyrrole, 10 mM LiI, and different TsOH concentration of (a) 0.1; (b) 0.5; (c) 1.0; and (d) 2.0 M. Insets correspond to the respective zoom-in images. The (e) is the one prepared with 0.2 M TsOH without addition of iodine species, while (f) is side view of film (d). The (g) is schematic diagram of formation of PPy thin film, not to scale.

3.3. Conductivity and electrocatalytic activity of PPy thin films

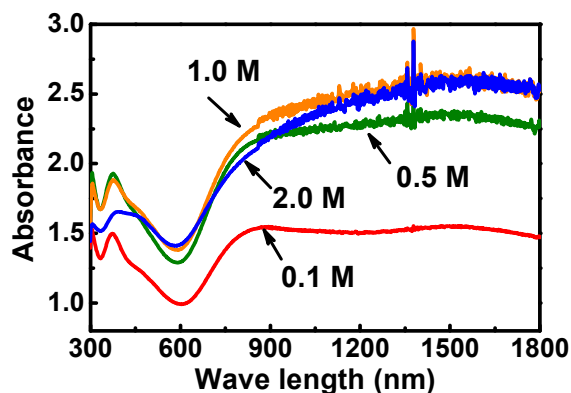


Fig. 3 Absorption spectra of as-prepared PPy films polymerized with 0.1 M pyrrole, 10 mM LiI and different concentrations of TsOH.

The conductivity of as-prepared PPy films was studied by vis-NIR absorption spectra (**Fig. 3**). The peak at around 380 nm is ascribed to the presence of I_3^- species in the film. The peak at around 480 nm is associated with $\pi-\pi^*$ electron transition of conjugated PPy chains, which can be attributed to the doping of TsO^- and/or iodine species.²⁵ The peak in NIR region from 850 to 1550 nm represents the electron transition from valence band to bipolaron band of the conjugated PPy chain, which reflects the delocalized polarons of PPy chains.²⁶ A red shift of the NIR absorption corresponds to a longer conjugation length of PPy chain and a more delocalized polarons. Thus, the conjugation length of PPy chain increases with the increasing concentration of TsOH, especially from 1.0 to 2.0 M. The ratio of the absorption peak in the NIR region to absorption peak around 480 nm can be used to represent the doping degree (i.e., conductivity) of PPy chains with TsO^- and iodine species.²⁷ A higher ratio represents a higher doping level of PPy chains, contributing to a higher conductivity. Since the ratio generally increases with the increasing concentration of TsOH (1.19, 1.37, 1.51, and 1.60), introduction of a higher concentration of TsOH results in a higher conductivity of PPy films. In addition, it is noted that a noise-like fluctuation at NIR region can be observed in the spectra, specifically at a relatively high concentration of TsOH (such as 0.5 M and above). This is possibly due to the interference and/or diffraction of light, which is closely to the film morphology. It may be also caused by some defects induced by the porous structure of PPy films.

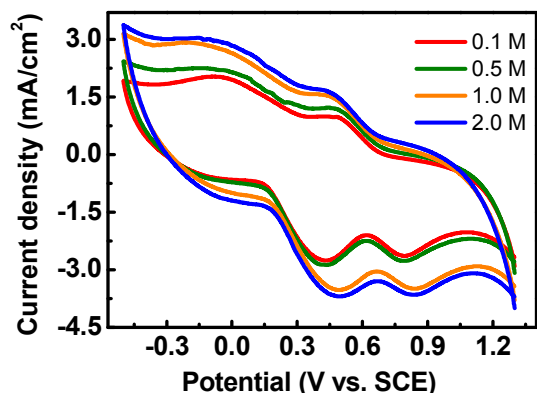


Fig. 4 CV curves of I^-/I_3^- redox couples on the as-prepared PPy films polymerized with 0.1 M pyrrole, 10 mM LiI and different concentrations of TsOH. The scan rate for CV is $50 \text{ mV}\cdot\text{s}^{-1}$.

The electrocatalytic activity of PPy films was studied first by CV technique. Two pairs of redox peaks can be observed in the spectra (**Fig. 4**). One is at ~ -0.05 and ~ 0.45 V, and another is at ~ 0.55 and ~ 0.75 V. The former corresponds to the redox of I^-/I_3^- couples, and the latter is the redox of I_3^-/I_2 couples.²⁸ The absolute value of peak current density for the oxidation of I^- is always slightly higher than that of the corresponding reduction of I_3^- for the same PPy electrode. So the oxidation of iodide is easier than the reduction of iodine on the surface of PPy electrodes, possibly because the I_3^- ions interact with PPy deeply inside the polymer chains.²⁸ Thus, it is important to improve the reduction

capability of iodine species on PPy electrode that has a great impact on the CE performance, which is dependent on the overpotential of PPy CEs. The value of open circuit voltage of PPy electrode (NOT the cell V_{OC}) was used to evaluate the overpotential approximately, which is 103.5, 94.5, 89.6, and 86.5 mV, respectively, for the respective TsOH concentration of 0.1, 0.5, 1.0, and 2.0 M. For comparison, it is 83.0 mV for Pt electrode. So the overpotential of PPy CEs decreases with increasing concentration of TsOH, resulting in an enhancement of the reduction capability of iodine species on PPy CEs. Moreover, the current density for both reduction and oxidation peaks of Γ/I_3^- couples, as well as the peak area corresponding to coulometric charge of electrochemical reaction, increases with increasing TsOH concentration. Thus, the PPy films prepared at high TsOH concentrations exhibit better electrocatalytic activity. In addition, the reduction-peak potential shifts to more negative values with increasing TsOH concentration, which agrees with the trend for the V_{OC} of DSSCs.

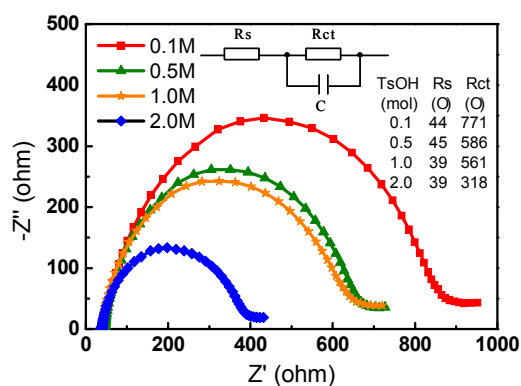


Fig. 5 EIS of DSSCs with different CEs measured under frequency of 0.01 Hz ~ 100 kHz. Inset shows the equivalent circuit and the calculated values for R_s and R_{ct} .

It is noted that the EIS can afford the information about resistance of charge transfer (R_{ct}) at the interface between the electrode and electrolyte, which is closely related to the electrocatalytic activity too and is thus studied here (**Fig. 5**). The R_{ct} reflects the one for the whole device, i.e., including both working and counter electrodes. It is noted that theoretically two semicircles should be observed in the EIS curve. One corresponds to the process at the interface between counter electrode and electrolyte (at high frequency) and another is the one between photoanode and electrolyte (at low frequency).^{29,30} Although in our work a small semicircle at high frequency can be observed (see Supporting Information), here it is not used for simulation as it is not well shaped. Since the TiO_2 photoanode is the same for all of the DSSCs, in addition, the change in R_{ct} can be mainly attributed to the change in PPy CEs, which is thus used to evaluate the electrochemical reaction resistance of a counter electrode in real working conditions. It is found from Fig. 5 that the R_{ct} decreases with the increase of TsOH concentration. So the charge transfer at the interface between PPy CE and electrolyte and, thereby, the electrocatalysis can be generally promoted by increasing TsOH concentration. This change trend agrees well with the above results of CV.

In addition, the amount of effective active sites in film taking

part in the electrocatalytic reactions, rather than the surface area, can also be used to describe the electrocatalytic property, which is evaluated by the value of double-layer capacitance of the interface between PPy film and electrolyte.³¹ The one for the Pt electrode is used as the reference. The respective ratio between these two is 2.47, 2.57, 2.84, and 3.84 for the TsOH concentration of 0.1, 0.5, 1.0, and 2.0 M, respectively. So the ratio increases with increasing TsOH concentration. A high ratio means a large amount of active sites in the film and, accordingly, more active of the electrocatalytic activity. This agrees well with the above conclusion.

3.4. Existing states of iodine species in PPy thin films

The above discussions can (partly) explain why the device performance changes with the change of TsOH concentration. But the working mechanism of CEs is still not clear. XPS spectra were thus collected and corresponding qualitative analysis results of as-prepared PPy films were shown in **Table 1** (more details refer to Supporting Information). The characteristic binding energy at ~ 400.4 eV ($N1s$), 168.1 eV ($S2p$), and 616.0~636.0 eV ($I3d$) originates from the N in the pyrrole rings, S in the TsO^- counter-anions, and I in the iodine species that existing in PPy films, respectively. So both TsO^- and iodine species are successfully doped/adsorbed in the polymer chain, which agrees with the above vis-NIR absorption results. The respective number of TsO^- counter ions per 10 pyrrole units (S_D) is 1.95, 2.88, 3.24, and 3.31 when the concentration of TsOH is 0.1, 0.5, 1.0, and 2.0 M, respectively. That is to say, the amount of doped TsO^- increases sharply at low concentration of TsOH, and then gradually tends to a constant when the concentration further increases from 1.0 to 2.0 M. Hence, the saturation doping is ~ 3 TsO^- ions per 10 pyrrole units, similar to the value given in the literature.²⁴

Table 1 XPS qualitative analysis results of as-prepared PPy films.

[TsOH]	[LiI]	Area percentage of $I_{3d5/2}$ XPS spectra (%)			$N_D/S_D/I_D$
		N_D	S_D (TsO^-)	I_D (I_k^-)	
0.1 M	0.01 M	19.4	35.5	3.6	10:1.95:1.64
0.5 M	0.01 M	14.0	37.9	5.8	10:2.88:0.83
1.0 M	0.01 M	12.9	36.3	7.3	10:3.24:0.78
2.0 M	0.01 M	8.7	40.0	8.4	10:3.31:0.91

It is noted that CV treatment can be used to imitate real working conditions of a CE in a DSSC cell. More important, the existing states of iodine species in the PPy films can be determined using XPS spectra. Four pairs of doublet peak can be observed in the spectra after deconvolution (**Fig. 6** and Supporting Information), regardless of with electrochemical treatment or not for the PPy film, which are attributed to different existing states of iodine in the films. The binding energy of the $I_{3d5/2}$ peak is ~618.6 eV ($peak_1$), ~620.7 ($peak_2$), ~622.3 ($peak_3$), and ~623.9 ($peak_4$), respectively. The $peak_1$ and $peak_2$ are ascribed respectively to Γ^- and I_3^- weakly bonded (or adsorbed) to PPy chains ($PPy \dots \Gamma^-$ and $PPy \dots I_3^-$), possibly via van der Waals interaction, π -electron interaction, and the like.^{28, 32} The $peak_3$ and $peak_4$ are attributed

respectively to the Γ^- and I_3^- strongly bonded to PPy chains (i.e., as doping counter anions, $\text{PPy}-\Gamma^-$ and $\text{PPy}-\text{I}_3^-$) mainly via the electrostatic interaction. The corresponding percentage of peak area is denoted as S_1 , S_2 , S_3 and S_4 , respectively (**Table 2**). The S_1 decreases monotonously with the increasing TsOH concentration, whereas S_3 and S_4 increase monotonously. As for S_2 , it first increases with the increasing TsOH concentration, then decreases slightly at 1.0 M, and eventually increases again at 2.0 M. Thus, the introduction of TsOH is in favor of the formation of both strongly bonded $\text{PPy}-\Gamma^-$ and $\text{PPy}-\text{I}_3^-$ species, and possibly also for the formation of weakly bonded $\text{PPy}\dots\text{I}_3^-$, while inhibits the formation of weakly bonded $\text{PPy}\dots\Gamma^-$. As the value of (S_2+S_4) is always much higher than that of (S_1+S_3) at the same TsOH concentration, the majority of iodine species exist in the oxidation state ($\text{PPy}-\text{I}_3^-$ and $\text{PPy}\dots\text{I}_3^-$) than the reduction state ($\text{PPy}-\Gamma^-$ and $\text{PPy}\dots\Gamma^-$). Specifically, the amount of $\text{PPy}\dots\text{I}_3^-$ species (S_2) are always much higher than the others at the same concentration, followed by the $\text{PPy}\dots\Gamma^-$ species (S_1). So lots of I_3^- species can be pre-stored as $\text{PPy}\dots\text{I}_3^-$ in the as-prepared PPy thin films.

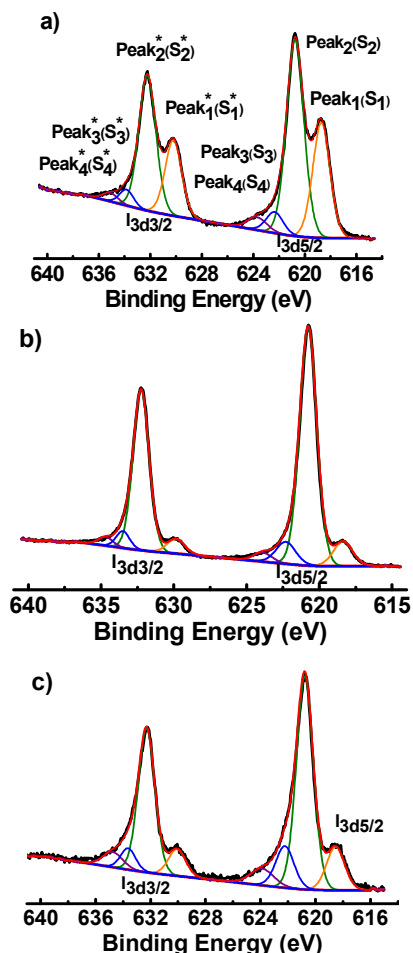


Fig. 6 $\text{I}_{3d3/2}$ and $\text{I}_{3d5/2}$ XPS spectra of PPy film polymerized with 0.1 M TsOH (a) without and (b) after CV treatment; (c) PPy film was polymerized with 2.0 M TsOH without CV treatment. CV treatment was carried out with a potential window between 1.3 and -0.5 V in acetonitrile solution containing 0.1 M LiClO_4 , 10 mM LiI , and 1 mM I_2 . The starting and end potential is -0.5 V.

Table 2 Area percentage of $\text{I}_{3d5/2}$ XPS spectra of as-prepared PPy films polymerized with different TsOH concentration.

Concentration of TsOH ^{a)}	Area percentage of $\text{I}_{3d5/2}$ XPS spectra (%)					
	S1	S2	S3	S4	S1 + S3	S2 + S4
0.1 M ^{a)}	19.4	35.5	3.6	2.5	23.0	38.0
0.5 M ^{a)}	14.0	37.9	5.8	2.6	19.8	40.5
1.0 M ^{a)}	12.9	36.3	7.3	3.5	20.2	39.8
2.0 M ^{a)}	8.7	40.0	8.4	4.3	17.1	44.3
0.1 M ^{b)}	5.8	49.0	5.2	2.0	11.0	51.0

^{a)} and ^{b)}: before and after the CV treatment.

The existing states of S_2 and S_3 increase obviously after CV treatment, while S_1 and S_4 decreases greatly (**Table 2**). So the increased weakly-bonded I_3^- species are mainly from the weakly-bonded Γ^- species as S_1 decreases from 19.4% to 5.8% after CV treatment and S_4 decreases from 2.5% to 2.0%. Moreover, the value of each existing state for the sample prepared with 0.1 M TsOH and after the electrochemical treatment is similar to that for the sample prepared with 2.0 M TsOH without the CV treatment (**Fig. 6b, c, Table 2**). That is to say, similar to the case for the PPy film prepared at a high TsOH concentration, large amount of iodine species (specifically the weakly-bonded I_3^- species) are formed in the film after electrochemical treatment (i.e., operation cycles of a real DSSC). This implies that the pre-stored $\text{PPy}\dots\text{I}_3^-$ in the as-prepared PPy thin film can participate in the electrochemical reduction occurring on the CEs when the film is assembled as a CE in a DSSC. This will lead to an easy and fast interfacial ion-exchange and/or charge transfer and, therefore, an improvement of the cell performance. Furthermore, it suggests that the active sites in polymer and, thereby, the electrocatalytic activity of the CEs are mainly determined by the weakly-bonded species (both $\text{PPy}\dots\text{I}_3^-$ and $\text{PPy}\dots\Gamma^-$), while the conductivity of resultant polymer is due to the strongly-bonded doping species.

3.5. Working mechanism of the CEs

In the electrolyte of DSSCs, iodine species exist mainly in the form of triiodide (I_3^-) via the reaction between I_2 and Γ^- (Equation 1), which can be reduced into Γ^- on the CEs. This is manifested by the observed yellow color of the polymerization solution (**Fig. 2g**). Electrons can transfer from the Γ^- ions in electrolyte to the photooxidized dye during cell operation (i.e., dye regeneration). The working mechanism of the CEs can thus be proposed (**Fig. 7**).

Totally three steps are involved in the electrocatalytic process. The first is formation of weakly and strongly bonded iodine species at the active sites during the cell operation (Equation 2-5). The second is the formation of electric neutral $\text{PPy}\dots\text{I}_2$ intermediates, which is realized mainly via the dissociation of $\text{PPy}\dots\text{I}_3^-$ and $\text{PPy}-\text{I}_3^-$ (Equation 6 and 7) and possibly via direct adsorption of I_2 molecules on the N center in PPy too (Equation 8). The last step is the reduction of $\text{PPy}\dots\text{I}_2$ into the reduction intermediate of $\text{PPy}\dots\text{I}$ on the CEs (Equation 9), which can be further reduced (Equation 10), resulting in the release of Γ^- ions into the electrolyte. These released Γ^- ions can form the I_3^- ions again (Equation 1) and/or form the $\text{PPy}\dots\Gamma^-$ (Equation 3) and $\text{PPy}-\Gamma^-$ (Equation 4). There is also a chance for $\text{PPy}-\text{I}_3^-$ to be dissociated into $\text{PPy}-\Gamma^-$ and I_2 (Equation 11). The $\text{PPy}-\Gamma^-$ can be produced by the reduction of $\text{PPy}\dots\text{I}$ too (Equation 12). Thus, the

PPy-I⁻ species increase upon the cell operation, while the PPy-I₃⁻ species decrease (Table 2). In addition, many of the PPy...I⁻ species can change into PPy...I₃⁻ during the cell operation (Equation 13), which then take part in the electrocatalytic process again. This explains why the PPy...I⁻ species decrease greatly upon the cell operation, while the PPy...I₃⁻ species increase obviously (Table 2). It is suggested that the formation of weakly-bonded species may be widely present for the CEs prepared with different types of materials, not just for PPy CEs, which determines the electrocatalytic activity of the CEs. Thus, the reactions participated by the weakly-bonded species can take place on different CEs. Moreover, Equation 2, 6, 9, and 10 may represent the major reactions occurring on these CEs. It is noted that the mechanism proposed herein is different from the one for the Pt CE (adsorption and oxidation of I⁻, and production of I₂ and I₃⁻).²³ Furthermore, the polymer exhibits unique properties as a CE material. For instance, the strongly bonded species are formed (Equation 4 and 5), which can modulate the CE conductivity and contribute to the electrocatalysis too (such as Equation 7). The resultant PPy...I₃⁻ species can be pre-stored in the film due to the polymer nature as well as the porous structure of film, while the latter is also in favor of the ion diffusion.

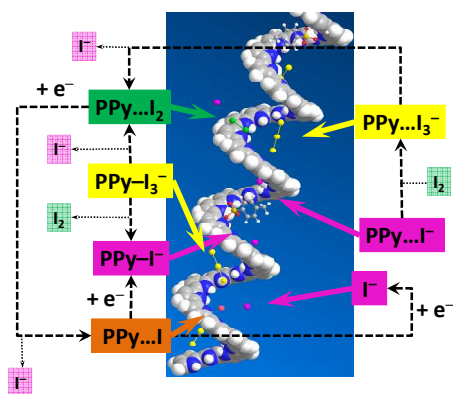


Fig. 7 Schematic diagram of the proposed working mechanism of PPy CEs in DSSCs.

The observed performance of DSSCs can thus be explained. When TsOH concentration is relatively low (such as 0.5 M and below), the porous structure, conductivity and active sites (electrocatalysis) of PPy films increase with the increase of its concentration (Fig. 8), resulting in an increase in the PCE of DSSCs based on the PPy CEs. Here the pre-stored PPy...I₃⁻ species may play a minor role. Once the concentration further increases to ~ 1.0 M, the PCE of resultant DSSC decreases possibly mainly due to the decrease in the amount of (pre-stored) PPy...I₃⁻ species, though the conductivity and active sites of the polymer still keep increasing slightly (Fig. 8). When the TsOH concentration increases to ~ 2.0 M, the active sites increase greatly and the polymer conductivity also increases (Fig. 8). Furthermore, the amount of (pre-stored) PPy...I₃⁻ species increases obviously at 2.0 M TsOH. Therefore, the PCE of the resultant DSSC increases. Further study is needed for the influence of film porosity on the DSSC performance when the TsOH concentration is relatively high (such 1.0 M and above). In addition, it is noted that the V_{OC} value of a DSSC is determined by the concentration of electron acceptors in the electrolyte.³³ Both the oxidized dye and I₃⁻ can act as such acceptors. A PPy CE with a high electrocatalytic activity is in favour of the I₃⁻ adsorption (both weakly and strongly) on the PPy CE, which can be reduced efficiently thereafter, resulting in a decrease in the concentration of I₃⁻ in the electrolyte. Therefore, the V_{OC} can be improved for a PPy CE with higher catalytic activity.³³ This may explain why the V_{OC} increases slightly with increasing TsOH concentration used for the preparation of PPy CEs (Fig. 1).

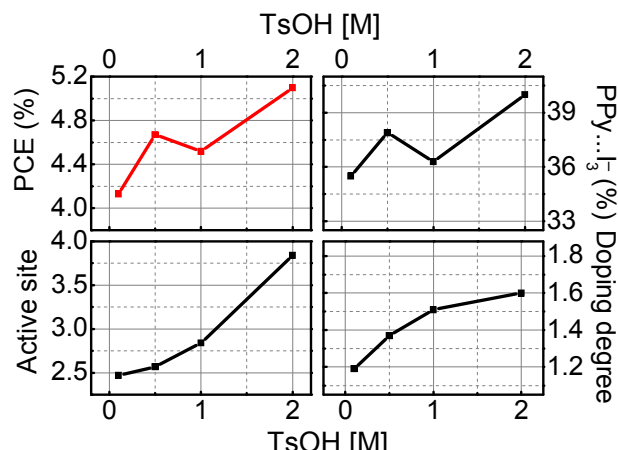


Fig. 8 The relationship between the PPy properties and the cell performance based on PPy CEs with different TsOH concentration.

70 Conclusions

In summary, we have demonstrated that the performance of the DSSCs based on PPy CEs is determined by the morphology, conductivity and electrocatalytic properties of the PPy films. The morphology is controlled by the concurrent electrochemical and chemical polymerization. The conductivity is mainly influenced by the strongly-bonded species. The electrocatalysis of the CEs is mainly determined by the weakly-bonded species, as well as the strongly-bonded species. In addition, some I₃⁻ species can be pre-stored in the as-prepared polymer films, which can take part in

the reduction of Γ/I_3^- redox couples later in a cell. The electrocatalytic mechanism of the CEs for I_3^- reduction in DSSCs is proposed for the first time. Totally three steps are involved, i.e., formation of the weakly and strongly bonded iodine species, formation of intermediates, and reduction of the intermediates as well as release of the Γ ions. This mechanism may also be valid for other CEs. Our results may have practical applications for the synthesis of alternative CEs. It may become even more interesting for the fabrication of (large-scale) flexible devices.

Acknowledgements

This work was supported by the Ministry of Science and Technology of China (2010DFB63530), and the Hundred-Talent Program of Chinese Academy of Sciences, National Natural Science Foundation of China (21203039).

Notes and references

^aNational Center for Nanoscience and Technology, Beijing 100190, China

^bUniversity of the Chinese Academy of Sciences, Beijing 100049, China
Fax: +86 10 6265 6765; Tel: +86 10 8254 5655;

E-mail: hei@nanoctr.cn, zhangxh@nanoctr.cn

^cDepartment of Chemistry, Tsinghua University, Beijing 100084, China

^dUniversity of Science and Technology Beijing, Beijing 100083, China

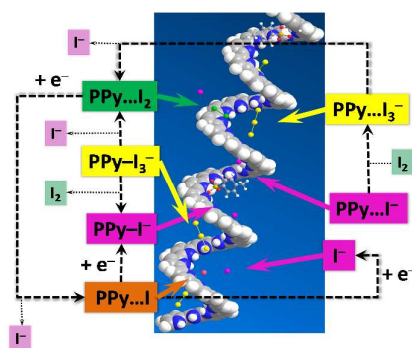
† Electronic Supplementary Information (ESI) available: [XPS spectra and iodine XPS spectra of as-prepared PPy films]. See DOI: 10.1039/b000000x/

- 1 B. O'Regan and M. Grätzel, *Nature*, 1991, **353**, 737.
- 2 E. J. W. Crossland, N. Noel, V. Sivaram, T. Leijtens, A. A. W. Jack and H. J. Snaith, *Nature*, 2013, **495**, 215.
- 3 A. Hagfeldt, G. Boschloo, L. Sun, L. Kloo and H. Pettersson, *Chem. Rev.*, 2010, **110**, 6595.
- 4 Y. Bai, J. Zhang, D. F. Zhou, Y. H. Wang, M. Zhang and P. Wang, *J. Am. Chem. Soc.*, 2011, **133**, 11442.
- 5 M. M. Lee, J. Teuscher, T. Miyasaka, T. N. Murakami and H. J. Snaith, *Science*, 2012, **338**, 643.
- 6 H. Gary and C. David, *Acc. Chem. Res.*, 2012, **45**, 705.
- 7 T. N. Murakami and M. Grätzel, *Inorg. Chim. Acta*, 2008, **361**, 572.
- 8 N. Papageorgiou, W. F. Mailer and M. Grätzel, *J. Electrochem. Soc.*, 1997, **144**, 876.
- 9 E. Olsen, G. Hagen and S. E. Lindquist, *Sol. Energy Mater. Sol. Cells*, 2000, **63**, 267.
- 10 M. K. Wang, A. M. Anghel, B. Marsan, N. L. Cevy Ha, N. Pootrakulchote, S. M. Zakkeeruddin and M. Grätzel, *J. Am. Chem. Soc.*, 2009, **131**, 15976.
- 11 F. Gong, H. Wang, X. Xu, G. Zhou and Z. S. Wang, *J. Am. Chem. Soc.*, 2012, **134**, 10953.
- 12 M. X. Wu, X. Lin, T. H. Wang, J. S. Qiu and T. L. Ma, *Energy Environ. Sci.*, 2011, **4**, 2308.
- 13 H. C. Sun, D. Qin, S. Q. Huang, X. Z. Guo, D. M. Li, Y. H. Luo and Q. B. Meng, *Energy Environ. Sci.*, 2011, **4**, 2630.
- 14 C. H. Xu, B. H. Xu, Y. Gu, Z. G. Xiong, J. Sun and X. S. Zhao, *Energy Environ. Sci.*, 2013, **6**, 1388.
- 15 H. N. Tian, Z. Yu, A. Hagfeldt, L. Kloo and L. C. Sun, *J. Am. Chem. Soc.*, 2011, **133**, 9413.
- 16 J. H. Wu, Q. H. Li, L. Q. Fan, Z. Lan, P. J. Li, J. M. Lin and S. C. Hao, *J. Power Sources*, 2008, **181**, 172.
- 17 Y. Hou, D. Wang, X. H. Yang, W. Q. Fang, B. Zhang, H. F. Wang, G. Z. Lu, P. Hu, H. J. Zhao and H. G. Yang, *Nat. Commun.*, 2013, **4**, 1.
- 18 S. S. Wang, S. Lu, X. M. Li, X. H. Zhang, S. T. He and T. He, *J. Power Sources*, 2013, **242**, 438.
- 19 L. X. Yi, Y. Y. Liu, N. L. Yang, Z. Y. Tang, H. J. Zhao, G. H. Ma, Z. Q. Su and D. Wang, *Energy Environ. Sci.*, 2013, **6**, 835.
- 20 H. Wang and Y. H. Hu, *Energy Environ. Sci.*, 2012, **5**, 8182.
- 21 P. Sudhagar, S. Nagarajan, Y. G. Lee, D. Song, T. Son, W. Cho, M. Heo, K. Lee, J. Won and Y. S. Kang, *ACS Appl. Mater. Interfaces*, 2011, **3**, 1838.
- 22 L. J. Chen, C. X. Guo, Q. M. Zhang, Y. L. Lei, J. L. Xie, S. J. Ee, G. H. Guai, Q. L. Song and C. M. Li, *ACS Appl. Mater. Interfaces*, 2013, **5**, 2047.
- 23 A. Hauch and A. Georg, *Electrochimica Acta*, 2001, **46**, 3457.
- 24 Y. F. Li and Y. F. Fan, *Synth. Met.*, 1996, **79**, 225.
- 25 K. Yakushi, L. J. Lauchlan, T. C. Clarke and G. B. Street, *J. Chem. Phys.*, 1983, **79**, 4774.
- 26 J. Lei, Z. Cai and C. R. Martin, *Synth. Met.*, 1992, **46**, 53.
- 27 J. Yong, O. Yang and Y. F. Li, *Polymer*, 1997, **38**, 1971.
- 28 H. Tang, A. Kitani and M. Shiotani, *J. Appl. Electrochem.*, 1996, **26**, 36.
- 29 Q. Wang, J. E. Moser and M. Grätzel, *J. Phys. Chem. B*, 2005, **109**, 14945.
- 30 A. Hauch and A. Georg, *Electrochim. Acta*, 2001, **46**, 3457.
- 31 A. J. Bard and L. R. Faulkner, *Electrochemical Methods, Fundamentals and Applications*, 6th ed., John Wiley & Sons, NJ, USA, 1998, pp 55–226.
- 32 C. D. Wagner, W. M. Riggs, L. E. Davis, J. F. Moulder and G. E. Muilenberg, *Handbook of X-ray Photoelectron Spectroscopy*, Perkin-Elmer, Minneapolis, USA, 1979, pp150-181.
- 33 C. C. Klark, G. J. Meyer, Q. Wei and E. Galoppini, *J. Phys. Chem. B*, 2006, **110**, 11044.

Working mechanism and performance of polypyrrole as counter electrode for dye-sensitized solar cells

Shan Lu, Shasha Wang, Xuemin Li, Ting Feng, Lingju Guo, Xuehua Zhang, Dongsheng Liu
and Tao He

Table of contents entry:



Electrocatalysis of PPy CEs mainly includes formation of weakly and strongly bonded iodine species, and formation and reduction of intermediates.